Check for updates

AGU ADVANCING EARTH AND SPACE SCIENCE

Geophysical Research Letters

RESEARCH LETTER
10.1029/2021GL094578

Key Points:

- The western North Pacific (WNP) tropical cyclone activity was a record low in early summer 2020 with only one short-lived tropical storm
- The Indian Ocean basin experienced a remarkable warming, unfavorable for cyclogenesis over the western North Pacific
- The simultaneous quasi-stationary MJO activity caused unfavorable background condition, causing the extremely inactive cyclogenesis

Supporting Information:

Supporting Information may be found in the online version of this article.

Correspondence to:
W. Zhang,
zhangwj@nuist.edu.cn

Citation:
Liu, C., Zhang, W., Jiang, F., Stuecker, M. F., & Huang, Z. (2021). Record-low WNP tropical cyclone activity in early summer 2020 due to Indian Ocean warming and Madden-Julian Oscillation activity. *Geophysical Research Letters*, *48*, e2021GL094578. https://doi.org/10.1029/2021GL094578

Received 28 MAY 2021
Accepted 30 JUN 2021

© 2021. American Geophysical Union. All Rights Reserved.

Record-Low WNP Tropical Cyclone Activity in Early Summer 2020 due to Indian Ocean Warming and Madden-Julian Oscillation Activity

Chao Liu[1], Wenjun Zhang[1], Feng Jiang[1], Malte F. Stuecker[2], and Zongci Huang[1]

[1]CIC-FEMD/ILCEC, Key Laboratory of Meteorological Disaster of Ministry of Education (KLME), Nanjing University of Information Science and Technology, Nanjing, China, [2]Department of Oceanography & International Pacific Research Center (IPRC), School of Ocean and Earth Science and Technology (SOEST), University of Hawai'i at Mānoa, Honolulu, HI, USA

Abstract During early boreal summer 2020, the western North Pacific (WNP) was characterized by record-low tropical cyclone (TC) activity, reaching the lowest historical level since 1979. Only one short-lived TC was observed in June and the whole of July underwent an unprecedented quiescent TC period. Concurrent Indian Ocean warming provided unfavorable conditions for cyclogenesis over the WNP, which partly (~40%) explains the extremely low TC number from a statistical standpoint. Accompanied with the Indian Ocean warming, an unprecedentedly long-lasting Madden-Julian Oscillation (MJO) event stalled over the Indian Ocean sector, persisting almost through the entire June and July. This simultaneous quasi-stationary MJO activity further caused unfavorable background conditions for cyclogenesis in the WNP. The Indian Ocean warming combined with the anomalous MJO conditions together largely (>80%) explain the record-low TC number over the WNP during early summer 2020.

Plain Language Summary Tropical Cyclone (TC) is one of the most intense storm systems with considerable socioeconomic impacts. Near one-third of global TC forms in the western North Pacific (WNP), the largest breeding ground for TCs on the planet. Climatologically, the active TC season starts from boreal early summer when background environments are favorable for TC formation. During early summer 2020, however, the WNP remains in an almost quiet state and the TC frequency sank to the lowest level on record since 1979. The physical processes responsible for it remain unclear. Accompanied with this extremely low TC frequency, the Indo-Pacific Oceans are characterized by strong Indian Ocean basin warming and ongoing La Niña development in the equatorial eastern Pacific. The large-scale tropical SST conditions provide unfavorable environment background for cyclogenesis and statistically explain about 50% of the extremely low TC frequency. Simultaneously, an unprecedentedly long-stalled Madden-Julian Oscillation (MJO) event was observed in the Indian Ocean. The MJO further worsens the background conditions for cyclogenesis and additionally explains above 40% of the record-low TC frequency. We here demonstrated that the record-low TC frequency in early summer 2020 is due to the combined effects of large-scale tropical SST conditions and the extraordinary MJO event.

1. Introduction

The western North Pacific (WNP; 0°N–40°N, 100°E–180°), the most active basin for tropical cyclone (TC) activity on the planet, witnesses one-third of global TCs each year on average. The typical TC season in the WNP usually spans from June to November, when both thermodynamic (e.g., sea surface temperature (SST) and mid-level moisture) and dynamic (e.g., vertical wind shear and low-level vorticity) conditions are favorable for TC formation (Li & Zhou, 2018). During summer 2020, the WNP TC activity experienced an extremely unusual behavior with the active TC season being postponed till August. Only one short-lived TC formed in June and the whole of July underwent an unprecedented quiescent TC period, which together brings down the total TC number in early summer (June-July) to the lowest historical level ever achieved since 1979. Investigations on the possible mechanisms that led to the record-low TC activity are of vital importance for the potential predictability of future similar extreme climate events.

As the predominant predictability source of global climate interannual variability, El Niño-Southern Oscillation (ENSO) strongly modulates the year-to-year variation of the WNP TC activity (e.g., Camargo

19448007, 2021, 14, Downloaded from https://agupubs.onlinelibrary.wiley.com/doi/10.1029/2021GL094578 by CochraneChina, Wiley Online Library on [14/11/2026]. See the Terms and Conditions (https://onlinelibrary.wiley.com/terms-and-conditions) on Wiley Online Library for rules of use; OA articles are governed by the applicable Creative Commons License

et al., 2007; G. Chen & Tam, 2010; Kim et al., 2011; B. Wang & Chan, 2002). During the developing year summer of an El Niño, the cyclogenesis over the WNP exhibits a dipole anomaly pattern with increased and decreased TC formation in the southeastern and northwestern quadrants, respectively. Roughly the opposite situation occurs during La Niña events. Therefore, the ENSO mainly influences the spatial distribution rather than the basin-wide TC genesis frequency during its developing phase (e.g., Chan, 1985; Chia & Ropelewski, 2002; Kim et al., 2011; B. Wang & Chan, 2002). The basin-wide cyclogenesis is usually decreased during the decaying early summer of traditional (eastern-Pacific, EP) El Niño events, due to the existence of strong low-level anticyclonic anomalies over the WNP (B. Wang & Chan, 2002). However, this negative relationship between TC frequency and preceding ENSO weakened in the recent two decades, when the central-Pacific (CP) El Niño occurred more frequently (e.g., Ashok et al., 2007; Kao & Yu, 2009; Kug et al., 2009; Ren & Jin, 2011; C. Wang et al., 2018). In contrast to the EP El Niño, CP El Niño normally witnesses weakly anticyclonic anomalies over the WNP during its decay summer based on the combination mode dynamics (Stuecker et al., 2013; W. Zhang et al., 2015). Concurrent with the record-low WNP TC activity in early summer 2020, the tropical Pacific experienced an ENSO phase transition from a weak CP warming to a weak EP cooling state. It seems that both the preceding CP El Niño event and the ongoing EP La Niña event are unlikely to explain the record-low TC frequency according to previous studies.

In addition to the tropical Pacific thermal condition, the remote Indian Ocean SST condition has also been demonstrated to exert an important role on the WNP TC activity (e.g., Du et al., 2011; Huangfu et al., 2019; Zhan et al., 2011). Pronounced Indian Ocean Basin warming (IOBM) usually follows the El Niño peak phase and persists toward boreal early summer, which can prolong ENSO's climate impacts over the WNP and surrounding regions via the so-called Indian Ocean Capacitor effect (Xie et al., 2009). The warm SST anomalies in the tropical Indian Ocean can force a warm tropospheric Kelvin wave that propagates into the western Pacific and influence the WNP summer cyclogenesis (Du et al., 2011; Xie et al., 2009). This type of Indian Ocean Capacitor effect is often evident following strong El Niño events. Despite the weak magnitude of the preceding El Niño event, strong warm SST anomalies were observed in the tropical Indian Ocean during the early summer of 2020, which could have provided unfavorable background for the WNP cyclogenesis. A few parallel independent studies have suggested a critical role of the tropical Indian Ocean on this record-low TC activity (C. Wang, Wu, et al., 2021; C. Wang, Yao, et al., 2021), its quantitative contribution, however, remains elusive.

Concurrent with the remarkable SST anomaly in the Indian Ocean, a unique stationary Madden–Julian Oscillation (MJO) event was identified based on the commonly-used MJO index, with the convective center long stalling over the tropical Indian Ocean. A typical MJO event usually initiates over the western Indian Ocean, propagates eastward through the Maritime Continent to the central Pacific, and dissipates near the dateline (Madden & Julian, 1971). Although the physical mechanisms governing this extraordinary MJO event are unclear, its pronounced impacts on plum rainfall have been felt over the adjacent regions (W. Zhang et al., 2021). Many previous studies have shown that the MJO can regulate the basin-wide TC frequency over the WNP by exciting the wave activity (e.g., G. Chen & Huang, 2008; Hall et al., 2001; Hartmann & Maloney, 2001; Li & Zhou, 2013; Madden & Julian, 1971). Therefore, it is compelling to hypothesize a potential contribution from this persistent MJO event to the extremely low TC frequency observed during the early summer of 2020.

At present, the physical mechanism for the record-low TC frequency during early summer 2020 remains to be understood. In this study, reanalysis datasets and statistical methods are used to elucidate the main physical forcing responsible for the record-low TC frequency during early summer 2020. We find that the extremely low TC frequency can be largely explained by the collective roles of the Indian Ocean basin warming and the superimposed extraordinary MJO event.

2. Data and Methodology

The atmospheric reanalysis dataset used in this study is derived from the NCEP-NCAR reanalysis (Kalnay et al., 1996), including monthly horizontal wind, and geopotential height. Monthly interpolated outgoing longwave radiation (OLR) provided by the National Oceanic and Atmospheric Administration (NOAA; Liebmann & Smith, 1996) is used as a proxy of deep convection. Global monthly mean SST is taken from

19448007, 2021, 14, Downloaded from https://agupubs.onlinelibrary.wiley.com/doi/10.1029/2021GL094578 by CochraneChina, Wiley Online Library on [14/11/2026]. See the Terms and Conditions (https://onlinelibrary.wiley.com/terms-and-conditions) on Wiley Online Library for rules of use; OA articles are governed by the applicable Creative Commons License

the NOAA Extended Reconstructed Sea Surface Temperature dataset, version 5 (Huang et al., 2017). The historical records for the WNP TC are derived from the Regional Specialized Meteorological Center (RSMC) Tokyo-Typhoon Center, Japan Meteorological Agency, which contains a complete history of the past estimates of storm's center locations, intensity, and other parameters at the six-hourly synoptic times. The daily real-time multivariate MJO (RMM; Wheeler & Hendon, 2004) index can be accessed from the Australian Bureau of Meteorology.

To quantify the modulation effect of MJO on WNP TC frequency, the daily genesis rate is used, which is defined as the number of TCs divided by the number of active MJO days in a particular phase. Following previous studies (Hall et al., 2001; Li & Zhou, 2013), the following statistical significance test is used to test for a statistical relationship between the MJO and the TC frequency:

$$Z = \frac{P - P_c}{\sqrt{P_c\left(1 - P_c\right) / N}}, \tag{1}$$

where P, P_c, and N represent daily genesis rate, climatology daily genesis rate, and the number of active MJO days under a particular MJO phase, respectively (see Text S1 in Supporting information for details). The test statistic Z follows a Gaussian distribution with the critical value of $Z = \pm 1.645$ at a 90% confidence level. All other statistical significance tests are performed based on the two-tailed Student's t-test. Throughout the manuscript, all anomalies were calculated as the departures from the climatological monthly mean from 1979 to 2019 and were linearly detrended.

3. Results

Figure 1a shows the seasonal evolution of the TC genesis number for the 2020 case with respect to climatology. During June-July 2020, only one short-lived tropical storm occurred in June and no TC was observed in July when climatological TC season begins. The cyclogenesis frequency did not restore to a normal condition until August, and the corresponding active TC season in 2020 has been postponed for two months compared to the climatology. The unusual behavior of the 2020 TC activity is clearly seen from the seasonal evolution of TC days as well (Figure 1b). We also examine the spatial distribution of TC genesis frequency and TC days anomalies, both of which exhibit consistent basin-wide decreases (Figure 1c, d). According to the time evolution of the historical June-July TC number, the year 2020 has reached the lowest historical level since 1979, which was previously achieved in 1998 (Figure 1e). This record-low TC frequency in early summer 2020 is also evident when extending the data back to the 1950s (Figure S1). Previous studies have shown that the basin-wide decrease of the WNP TC frequency in early summer is usually associated with an El Niño event in the previous winter (e.g., B. Wang & Chan, 2002; C. Wang et al., 2018), as represented by their out of phase inter-relationship ($R = -0.5$; Figure 1e). For example, no TC was observed over the WNP up to June in the years 1998 and 2016, following two extreme El Niño events (Figure S2). In response to the distinct evolution of subsequent Pacific SST states, the following TC activity exhibited salient different behaviors in these 2 years, which remained suppressed in 1998 and restored to normal condition in 2016 (Huangfu et al., 2018; Zhan et al., 2017). Preceded by a weak CP El Niño event during the 2019/2020 winter (Figure S3), the boreal summer condition of 2020, did not mimic those in 1998 and 2016, which was characterized by much earlier occurrence of the first WNP TC in May. The Pacific warm state in the previous winter is thus unlikely to be a statistical precursor of the such extreme low TC frequency given its magnitude and spatial distribution (B. Wang & Chan, 2002; C. Wang et al., 2018).

To inspect the possible causes, we next examine the large-scale SST, convection, and low-level circulation anomalies in early summer 2020 (Figure 2a, b). Conspicuous basin-wide SST warming and an ongoing La Niña occurred in the tropical Indian Ocean and tropical eastern Pacific, respectively. Superimposed on these SST anomalies, strongly enhanced and depressed convections were observed in the western Indian Ocean and western Pacific. Simultaneously, an intense low-level anticyclonic circulation anomaly was evident in the subtropical western Pacific, which covers most of the WNP and extends to the Indian peninsula. This anomalous anticyclonic circulation provided an unfavorable condition for cyclone genesis, including decreased middle-level moisture, enhanced vertical wind shear, and strong anticyclonic low-level vorticity (Figure S4). To examine the possible role of large-scale ocean-atmospheric states on the basin-wide

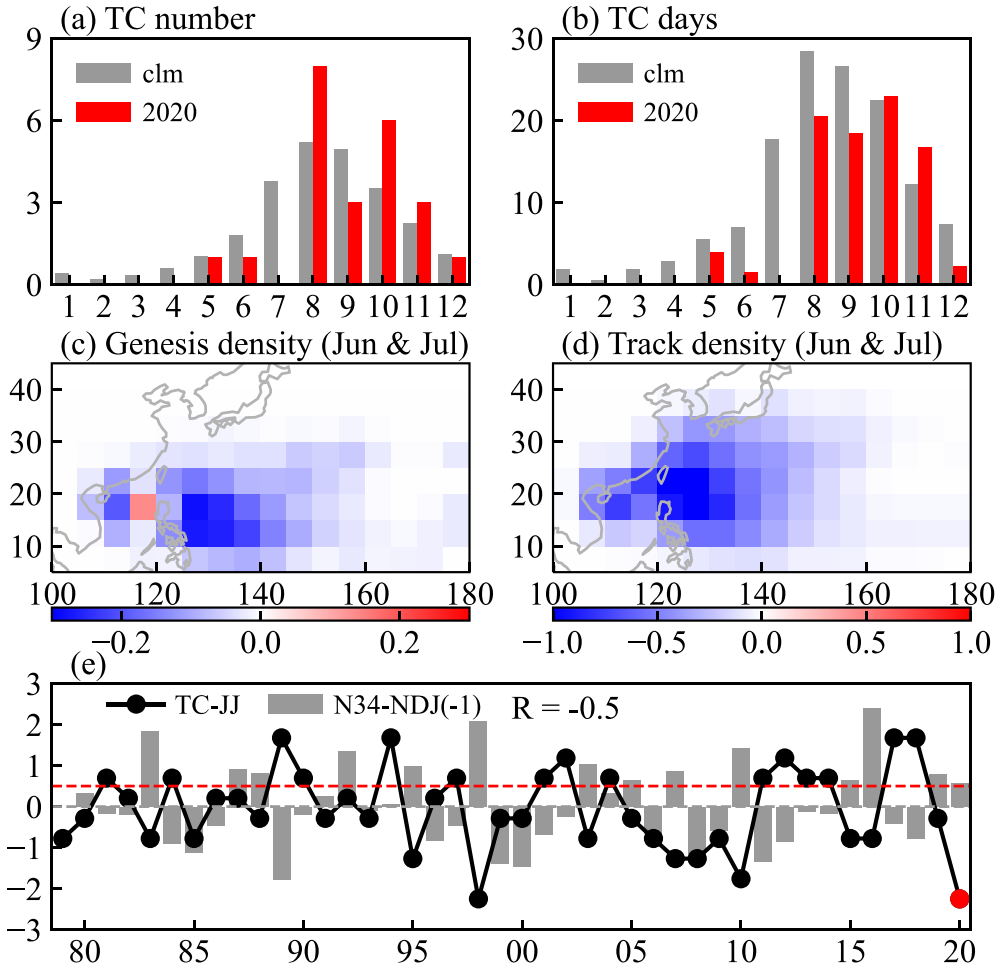


Figure 1. Monthly TC (a) genesis frequency and (b) days in 2020 (red) compared with the 1979–2019 climatological mean (gray). Spatial distribution of TC (c) genesis density (number per 5° × 5° grid) and (d) track density (days per 5° × 5° grid) anomaly during June-July 2020. (e) Time evolution of normalized June-July TC genesis frequency (mark line) and Niño3.4 (bars; 120°–170°W, 5°S–5°N) index in the preceding winter (November-December-January). TC genesis frequency in 2020 is highlighted by the red marker and the horizontal dashed line denotes the 0.5 standard deviations.

TC frequency variability, we show the spatial distribution of their correlation maps (Figure 2c, d). These correlation maps resemble the anomalous states observed in early summer 2020 and are not significantly altered if an additional month (i.e., May or August; Figure S5) is added in the analysis, indicating nonnegligible contributions of the large-scale ocean-atmospheric conditions to the extremely low TC frequency. Note that the sign of the correlation maps has been reversed for easy comparison. An anomalously warm Indian Ocean and cold tropical Pacific were also identified as important factors affecting the interannual variability of the East Asia summer monsoon (e.g., Kosaka et al., 2013; B. Wang et al., 2013; Xie et al., 2009). Considering the spatial distributions of the observed SST anomalies and the correlations maps, we here chose the IOBM and Niño3.4 indices to investigate possible contributions from the large-scale thermal condition concurrent with the extreme TC activity (Figure 2e). Both indices essentially reflect the respective leading statistical modes (i.e., Empirical Orthogonal Functions) of interannual climate variability in the two basins (e.g., Ashok et al., 2007; Yang et al., 2007). The influences of other higher order statistical modes are comparatively small either due to their small magnitudes in 2020 or their weak statistical relationships with WNP TC numbers (not shown). It is shown that the IOBM exhibits a complex relationship with simultaneous ENSO conditions during the early summer (R ~ 0.32). In some years (e.g., 1987, 2002, 2015), both of the IOBM and Niño3.4 show significant warm anomalies, however, almost opposite anomalies in sign occur in other years (e.g., 1988, 1998, and 2010). The overall weak inter-relationship between these two indices

19448007, 2021, 14, Downloaded from https://agupubs.onlinelibrary.wiley.com/doi/10.1029/2021GL094578 by CochraneChina, Wiley Online Library on [14/11/2026]. See the Terms and Conditions (https://onlinelibrary.wiley.com/terms-and-conditions) on Wiley Online Library for rules of use; OA articles are governed by the applicable Creative Commons License

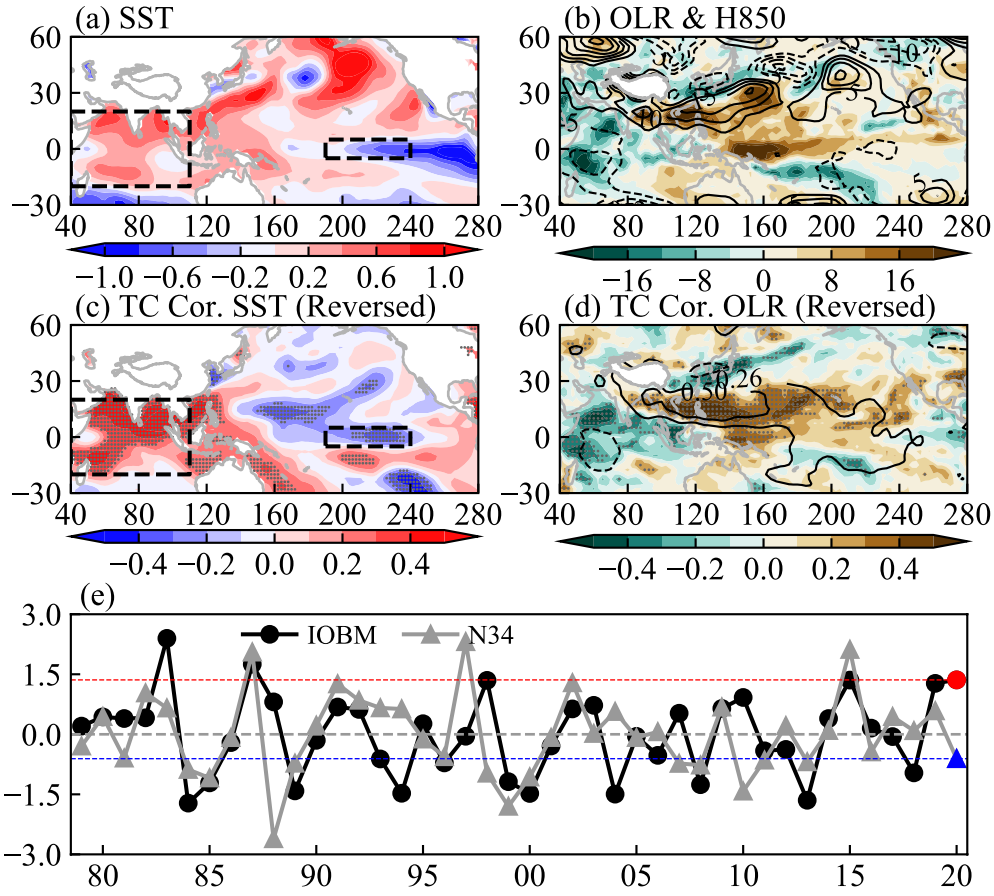


Figure 2. Spatial distribution of June-July averaged (a) SST (°C), (b) OLR (shading, W/m^2), and 850 hPa geopotential height (contours, m) anomalies in 2020. Correlation maps of basin-wide June-July TC frequency with simultaneous (c) SST, (d) OLR (shading), and 850 hPa geopotential height (contours). (e) Normalized time evolution of June-July averaged IOBM (40°–110°E, 20°S–20°N; black) and Niño3.4 (gray) indices, which are outlined by dashed boxes in (a) and (c). In (c) and (d), the signs of correlation coefficients have been reversed for comparison and only values exceeding the 90% confidence level are stippled (shading) or shown (contour). The red and blue markers, as well as horizontal dashed lines in (e), denote the IOBM and Niño3.4 condition in 2020, respectively.

suggests that their variability and potential roles for WNP TC activity are largely independent. During early summer 2020, an extremely strong IOBM (1.4 standard deviation) event occurred, ranking third in amplitude. In contrast, the ongoing La Niña was rather weak as measured by the Niño3.4 index (−0.59 standard deviation).

To measure the contribution of the Indo-Pacific SST conditions to the extremely low TC numbers, we construct a statistical binary regression model based on the standardized IOBM and Niño3.4 indices (TC = −1.24 × IOBM + 0.93 × Niño3.4; Figure 3a). The reconstruction has a reasonable skill in capturing the observed past TC variability (R = 0.63, statistically significant at the 95% confidence level) and the relationship is significant throughout almost the entire study period (Figure 3c). Despite that this statistical model captures a negative anomaly of TC frequency in 2020, it underestimates the observed anomaly by about half (−2.25 vs. −4.27%; 53%) (Figure 3b). The corresponding atmospheric fields reconstructed by the statistical model can also well reproduce the basic observational features, including zonal dipole structures of convection between the Indian Ocean and western Pacific, the strengthened low-level anticyclonic circulation over the WNP, and unfavorable environmental factors associated with cyclogenesis, but still suffer from the magnitude underestimation (Figures 3d and S6). The underestimated magnitude of circulation anomalies suggests that other physical processes independent of tropical ocean thermal conditions were at work as well, which will be discussed later. The statistical analyses shown here are also consistent with numerical model results displayed in other parallel independent studies (Takaya et al., 2020; C. Wang, Wu, et al., 2021;

19448007, 2021, 14, Downloaded from https://agupubs.onlinelibrary.wiley.com/doi/10.1029/2021GL094578 by CochraneChina, Wiley Online Library on [14/11/2026]. See the Terms and Conditions (https://onlinelibrary.wiley.com/terms-and-conditions) on Wiley Online Library for rules of use; OA articles are governed by the applicable Creative Commons License

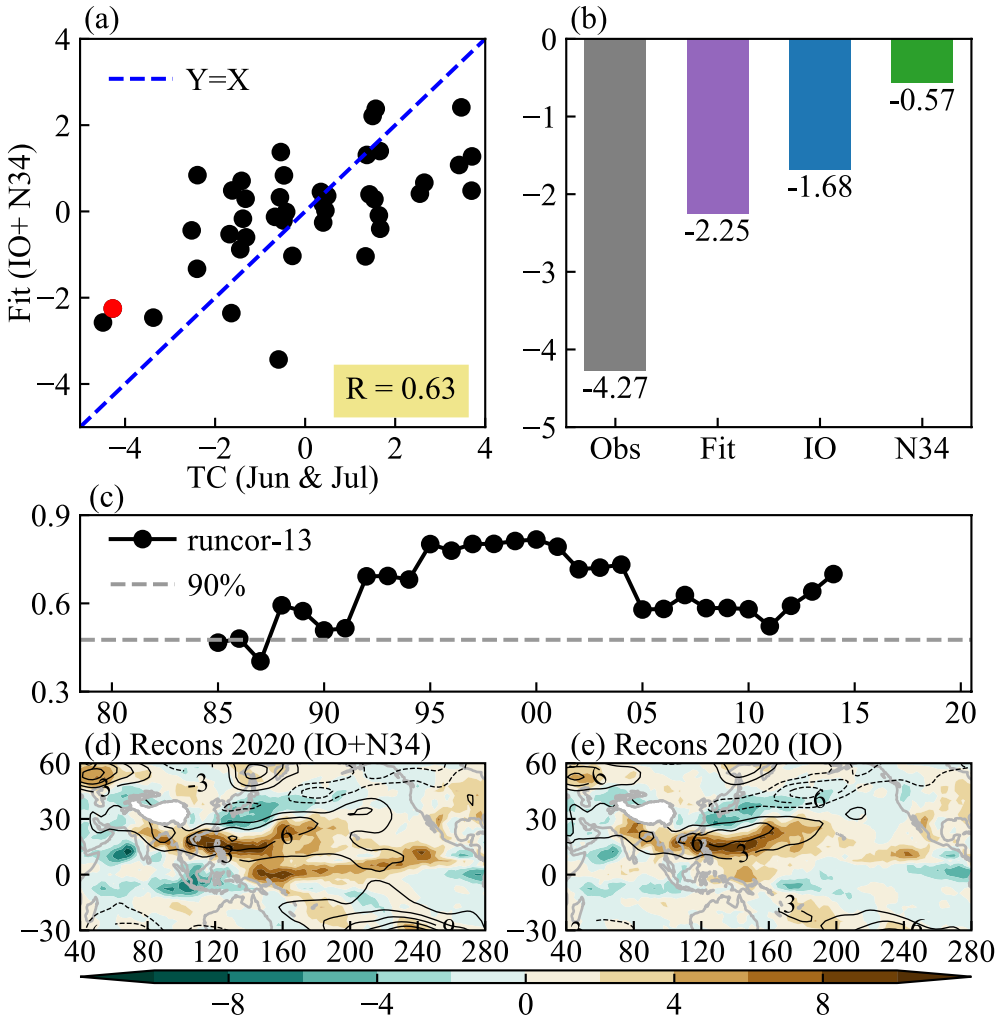


Figure 3. (a) Scatter plot between observed and statistical model reconstructed June-July TC genesis frequency anomaly. The red dot stands for the 2020 case. (b) The observed anomalous TC frequency in 2020 and the parts explained by different components of the statistical model. (c) Thirteen-year running correlation between the observed and model fitted TC genesis number (mark line). Spatial distribution of OLR (shading, W/m^2) and 850 hPa geopotential height (contours, m) reconstructed by the (d) full statistical model and (e) the IOBM. The dashed line in (a) and (c) represent the best-fit line and 90% confidence level, respectively.

Zhou et al., 2021), in which the magnitude of the anomalous large-scale WNP circulations forced by tropical ocean SST anomalies was about half of the observed anomalies. A further decomposition of the statistical model shows that the Indian Ocean warming played a major role (−1.68 vs. −4.27%; 40%) while the effect of La Niña was minor (−0.57 vs. −4.27%; 13%). A sensitivity analysis of the statistical model, such as varying training period and the number of months used for the seasonal mean, do not qualitatively alter the estimated contributions (Table S1). Importantly, the WNP strengthened low-level anticyclonic circulation was mainly contributed by the IOBM (Figure 3e), in accord with the primary role of IOBM on the TC frequency decrease. As suggested by previous studies, the IOBM can trigger a warm tropospheric Kelvin wave that propagates into the western Pacific, exciting the anomalous anticyclone and thus suppressing cyclogenesis (e.g., Du et al., 2011; Xie et al., 2009; Zhou et al., 2021). Therefore, we conclude that the large-scale Indo-Pacific SST state can explain about 50% of the extreme negative anomalies of TC frequency during early summer 2020 due to an adjustment of the WNP atmospheric circulation.

Interestingly, this unusual TC activity was also concurrent with an extraordinary long-stalled MJO event (Figure 4a), distinct from the eastward propagation features of typical MJO events. The unusual MJO is

19448007, 2021, 14, Downloaded from https://agupubs.onlinelibrary.wiley.com/doi/10.1029/2021GL094578 by CochraneChina, Wiley Online Library on [14/11/2026]. See the Terms and Conditions (https://onlinelibrary.wiley.com/terms-and-conditions) on Wiley Online Library for rules of use; OA articles are governed by the applicable Creative Commons License

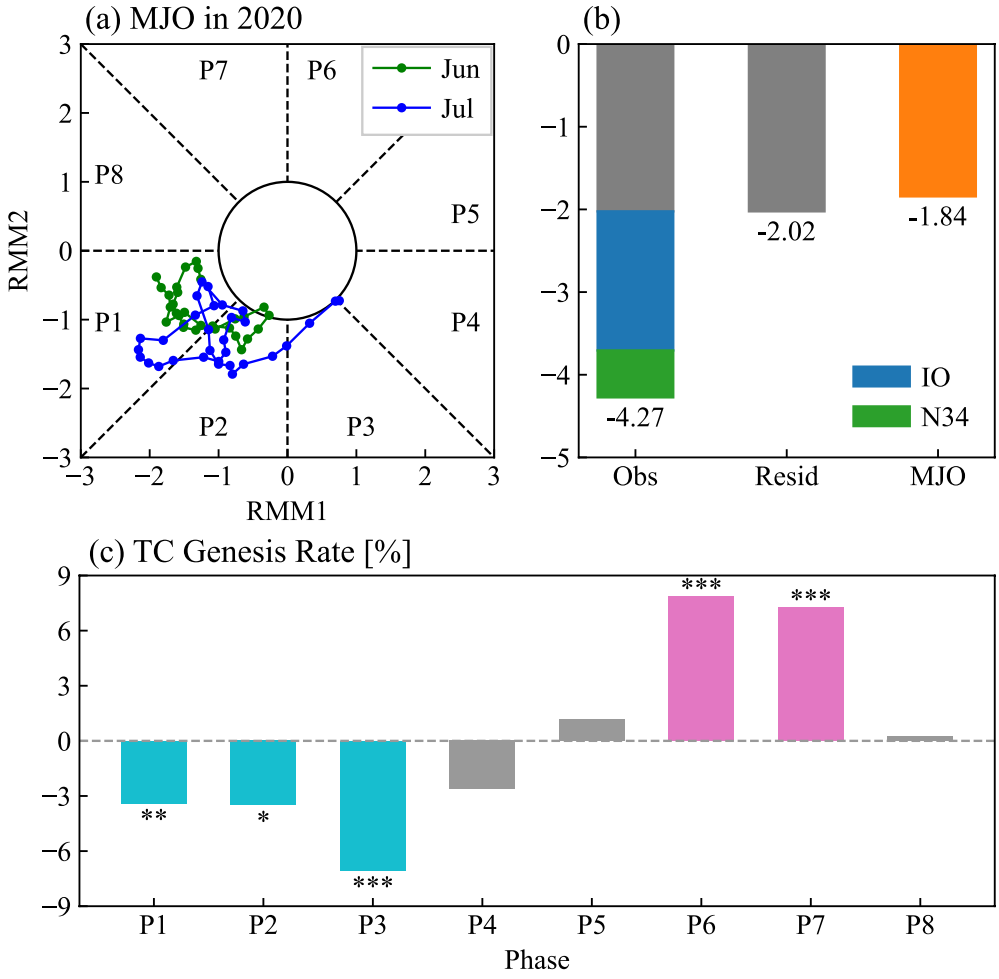


Figure 4. (a) MJO phase evolutions during the summer of 2020. The Green and the blue line indicate the period in June and July, respectively. (b) The observed anomalous WNP TC frequency in 2020, which is further decomposed into the components contributed by the IOBM, Niño3.4, and the residual term. The contribution of MJO active days in Phases 1–2 to the residual term is also shown. (c) Composite WNP TC daily genesis rate (day^{-1}) anomalies during different MJO phases. Values exceeding 85%, 90%, and 95% confidence levels are labeled with asterisk *, **, and ***, respectively.

characterized by persistently large RMM indices in Phases 1–2 (the tropical Indian Ocean) during June-July 2020. The active MJO days (RMM amplitude ≥ 1; 56 days) in Phases 1–2 during 2020 is the longest observed duration of the MJO in those two phases throughout the study period, much longer than the climatology (14 days; Figure S7). It has long been recognized that the MJO can exert a considerable modulation on cyclogenesis (e.g., Camargo et al., 2009; Diamond & Renwick, 2014; Li & Zhou, 2013; Moon et al., 2018). We here show the composite TC daily genesis rate anomalies for the eight MJO phases (Figure 4c). It is found that the WNP cyclogenesis exhibits a pronounced decrease and increase when the MJO is in Phases 1–3 and 6–7, respectively. To alleviate a possible interference from insufficient data sampling, we also examined the MJO's modulation effect on WNP TC days during the typical TC season (i.e., June to November) in the Northern Hemisphere and found nearly identical phase-dependent MJO-TC relationships (Figure S8). The MJO concomitant circulation anomalies over the WNP, such as low-level vorticity and vertical wind shear, can influence the synoptic-scale eddy barotropic energy conversion and further modulate the synoptic-scale activity and cyclogenesis according to previous studies (e.g., Hsu et al., 2017; Li & Zhou, 2013; Maloney & Hartmann, 2001; Moon et al., 2018; Figure S9). Considering the longest active MJO days in Phases 1–2 during early summer 2020 and the phase-dependent MJO-TC relationship, we hypothesize an important contribution of this quasi-stationary MJO on the extreme TC genesis frequency decrease. One recent study has also identified an active role of intra-seasonal variability in affecting the WNP anomalous anticyclone

19448007, 2021, 14, Downloaded from https://agupubs.onlinelibrary.wiley.com/doi/10.1029/2021GL094578 by CochraneChina, Wiley Online Library on [14/11/2026]. See the Terms and Conditions (https://onlinelibrary.wiley.com/terms-and-conditions) on Wiley Online Library for rules of use; OA articles are governed by the applicable Creative Commons License

during the summer season. Strong intra-seasonal variability can yield nonzero monthly means that project onto the anomalous anticyclone pattern (X. Wang et al., 2020). To quantify the MJO's effect, we regressed the TC frequency unexplained by the large-scale SST state (i.e., IOBM and Niño3.4) onto the accumulated active MJO days in Phases 1–2. The inclusion of MJO activity explains an additional 11% (statistically significant at 95% confidence level) of the June-July TC variability for the entire period (i.e., 1979–2020). For the 2020 extreme case (Figure 4b), the quasi-stationary MJO event contributed to 43% (−1.84 vs. −4.27) of the 2020 TC frequency anomaly, taking up most of the part unexplained by the large-scale SST conditions (−1.84 vs. −2.02). When the MJO moved eastward in August 2020, the associated suppression effect was largely weakened, which promoted a bloom of the WNP cyclogenesis.

4. Conclusion and Discussion

Despite the weak magnitude of El Niño in the preceding winter, the WNP TC activity exhibited an extreme decrease during early summer 2020, which has brought much public attention to TC variability and climate extremes. Concurrent with the record-low TC activity, anomalous strong basin-wide SST warming (third-ranking in amplitude) and an unprecedented long-stalled MJO event (top-ranking in persistence) were observed in the tropical Indian Ocean. We demonstrate that both of them significantly contributed to the extreme negative TC frequency anomaly. In contrast, the concurrent weak La Niña event in the tropical eastern Pacific played a relatively minor role. A contribution of tropical Oceans on the record-low TC activity is also in accord with a few parallel independent studies (C. Wang, Wu, et al., 2021; C. Wang, Yao, et al., 2021). On the basis of the large-scale SST conditions, we here further highlight that the unusual MJO related atmospheric variability needs to be considered in understanding the extreme WNP TC activity, especially on sub-seasonal timescales.

Compared to the 2020 case, the 1998 early summer also experienced a similar decreased TC activity (Figures S1 and S2a, b), which was accompanied by a comparable magnitude of IOBM and a slightly more negative Niño3.4 index (Figure 2e). The MJO's effect as represented by the residence time over the tropical Indian Ocean sector in early summer 1998 (5 days; Figure S7), however, was comparatively weak. Therefore, we hypothesize a difference of the leading physical processes in these two extreme years. Despite the comparable magnitude of tropical Indian Ocean warming, the tropical Pacific SST cooling center was located further westward in the early summer of 1998 (Figure S10). The westward shifted Pacific cooling in 1998 superimposed on the warm climatological SST induced a more intense WNP atmospheric responses, which compensated for the comparatively weak effect of the MJO in that year. The important role of tropical Pacific SST anomalies in 1998 early summer on WNP TC activity has been documented by several previous studies (Huangfu et al., 2018; Zhan et al., 2017). For the 2020 case, we hypothesize that the anomalous Pacific SST cooling played a minor role due to its further eastward located center. Thus, the strong low-level anti-cyclonic circulation anomalies over the WNP in 2020 were mainly contributed by the Indian Ocean warming and the superimposed long-stalled MJO event.

It is still a challenging task to predict extreme events more than two weeks in advance, due to the lack of dynamical understanding of such extreme events (e.g., N. Chen & Majda, 2015; Hsu et al., 2020). In this study, the 2020 extreme TC activity is taken as an example to explore the mechanisms driving this extreme climate event. However, the physical processes responsible for the exceptional quasi-stationary MJO event in early summer 2020 remain to be elucidated. One recent study showed that the MJO propagation pattern exhibits diversity and can be generally grouped into four archetypes (i.e., standing, jumping, slow east propagation, and fast east propagation; G. Chen & Wang, 2020). In particular, the MJO tends to be standing or slowly eastward propagating when cold SST anomalies occur in the central to eastern equatorial Pacific, suggesting possible modulation effects from the background SST state (e.g., G. Chen & Wang, 2020; B. Wang et al., 2019). We also examine the correlation map of accumulated MJO active days in Phases 1–2 with simultaneous SST anomalies (Figure S11). It is shown that a basin-wide warm SST background over the Indian Ocean could indeed be favorable for a quasi-stationary MJO. However, their statistical relationship is relatively weak ($R \sim 0.3$). Thus, we conclude that the positive IOBM does not necessarily guarantee the occurrence of a persistent MJO activity. During early summer 2020, the concurrent weak La Niña event in the tropical Pacific and positive SST anomalies in the Indian Ocean may have acted together to strengthen the Walker Circulation, thereby enhancing the easterly wind shear over Indo-Western Pacific and thus provided

19448007, 2021, 14, Downloaded from https://agupubs.onlinelibrary.wiley.com/doi/10.1029/2021GL094578 by CochraneChina, Wiley Online Library on [14/11/2026]. See the Terms and Conditions (https://onlinelibrary.wiley.com/terms-and-conditions) on Wiley Online Library for rules of use; OA articles are governed by the applicable Creative Commons License

an unfavorable large-scale environment for MJO eastward propagation (C. Zhang & Dong, 2004). A future in-depth investigation is necessary for a better dynamical understanding of this unprecedented MJO event and the potential predictability of similar extreme climate events.

Data Availability Statement

Reanalysis data sets used in this paper are available from https://psl.noaa.gov/data/gridded/data.noaa.ersst.v5.html, https://psl.noaa.gov/data/gridded/data.ncep.reanalysis.html, and https://psl.noaa.gov/data/gridded/data.interp_OLR.html. The historical tropical cyclone best-track data sets are located at https://www.jma.go.jp/jma/jma-eng/jma-center/rsmc-hp-pub-eg/besttrack.html. The RMM index is available at https://www.bom.gov.au/climate/mjo/graphics/rmm.74toRealtime.txt.

Acknowledgments
We thank the anonymous reviewers for their constructive comments and suggestions. This work was supported by the National Nature Science Foundation of China (42088101), the National Key Research and Development Program (2018YFC1506002), and the Innovation Project of Jiangsu Province (KYCX20_0913). MFS was supported by NOAA's Climate Program Office's Modeling, Analysis, Predictions, and Projections (MAPP) program grant NA20OAR4310445. This is IPRC publication 1529 and SOEST contribution 11371-.

References

Ashok, K., Behera, S. K., Rao, S. A., Weng, H., & Yamagata, T. (2007). El Niño Modoki and its possible teleconnection. *Journal of Geophysical Research*, *112*(C11). https://doi.org/10.1029/2006jc003798

Camargo, S. J., Emanuel, K. A., & Sobel, A. H. (2007). Use of a genesis potential index to diagnose ENSO effects on tropical cyclone genesis. *Journal of Climate*, *20*(19), 4819–4834. https://doi.org/10.1175/jcli4282.1

Camargo, S. J., Wheeler, M. C., & Sobel, A. H. (2009). Diagnosis of the MJO modulation of tropical cyclogenesis using an empirical index. *Journal of the Atmospheric Sciences*, *66*(10), 3061–3074. https://doi.org/10.1175/2009jas3101.1

Chan, J. C. L. (1985). Tropical cyclone activity in the northwest Pacific in relation to the El Niño/southern oscillation phenomenon. *Monthly Weather Review*, *113*(4), 599–606. https://doi.org/10.1175/1520-0493(1985)113<0599:tcaitn>2.0.co;2

Chen, G., & Huang, R. (2008). Influence of monsoon over the warm pool on interannual variation on tropical cyclone activity over the western North Pacific. *Advances in Atmospheric Sciences*, *25*(2), 319–328. https://doi.org/10.1007/s00376-008-0319-7

Chen, G., & Tam, C.-Y. (2010). Different impacts of two kinds of Pacific Ocean warming on tropical cyclone frequency over the western North Pacific. *Geophysical Research Letters*, *37*(1), L01803. https://doi.org/10.1029/2009gl041708

Chen, G., & Wang, B. (2020). Circulation factors determining the propagation speed of the Madden–Julian oscillation. *Journal of Climate*, *33*(8), 3367–3380. https://doi.org/10.1175/jcli-d-19-0661.1

Chen, N., & Majda, A. J. (2015). Predicting the real-time multivariate Madden–Julian oscillation index through a low-order nonlinear stochastic model. *Monthly Weather Review*, *143*(6), 2148–2169. https://doi.org/10.1175/mwr-d-14-00378.1

Chia, H. H., & Ropelewski, C. F. (2002). The interannual variability in the genesis location of tropical cyclones in the northwest Pacific. *Journal of Climate*, *15*(20), 2934–2944. https://doi.org/10.1175/1520-0442(2002)015<2934:tivitg>2.0.co;2

Diamond, H. J., & Renwick, J. A. (2014). The climatological relationship between tropical cyclones in the southwest pacific and the Madden-Julian Oscillation. *International Journal of Climatology*, *35*(5), 676–686. https://doi.org/10.1002/joc.4012

Du, Y., Yang, L., & Xie, S.-P. (2011). Tropical Indian Ocean influence on northwest Pacific tropical cyclones in summer following strong El Niño. *Journal of Climate*, *24*(1), 315–322. https://doi.org/10.1175/2010jcli3890.1

Hall, J. D., Matthews, A. J., & Karoly, D. J. (2001). The modulation of tropical cyclone activity in the Australian region by the Madden–Julian oscillation. *Monthly Weather Review*, *129*(12), 2970–2982. https://doi.org/10.1175/1520-0493(2001)129<2970:tmotca>2.0.co;2

Hartmann, D. L., & Maloney, E. D. (2001). The Madden–Julian Oscillation, barotropic dynamics, and north Pacific tropical cyclone formation. Part II: Stochastic barotropic modeling. *Journal of the Atmospheric Sciences*, *58*(17), 2559–2570. https://doi.org/10.1175/1520-0469(2001)058<2559:tmjobd>2.0.co;2

Hsu, P.-C., Lee, T.-H., Tsou, C.-H., Chu, P.-S., Qian, Y., & Bi, M. (2017). Role of scale interactions in the abrupt change of tropical cyclone in autumn over the Western North Pacific. *Climate Dynamics*, *49*(9–10), 3175–3192. https://doi.org/10.1007/s00382-016-3504-x

Hsu, P.-C., Qian, Y., Liu, Y., Murakami, H., & Gao, Y. (2020). Role of abnormally enhanced MJO over the western Pacific in the formation and subseasonal predictability of the record-breaking northeast Asian heatwave in the summer of 2018. *Journal of Climate*, *33*(8), 3333–3349. https://doi.org/10.1175/jcli-d-19-0337.1

Huang, B., Thorne, P. W., Banzon, V. F., Boyer, T., Chepurin, G., Lawrimore, J. H., et al. (2017). Extended reconstructed sea surface temperature, version 5 (ERSSTv5): Upgrades, validations, and intercomparisons. *Journal of Climate*, *30*(20), 8179–8205. https://doi.org/10.1175/jcli-d-16-0836.1

Huangfu, J., Chen, W., Huang, R., & Feng, J. (2019). Modulation of the impacts of the Indian Ocean basin mode on tropical cyclones over the northwest Pacific during the boreal summer by La Niña Modoki. *Journal of Climate*, *32*(11), 3313–3326. https://doi.org/10.1175/jcli-d-18-0638.1

Huangfu, J., Huang, R., Chen, W., & Feng, T. (2018). Causes of the active typhoon season in 2016 following a strong El Niño with a comparison to 1998. *International Journal of Climatology*, *38*(S1), e1107–e1118. https://doi.org/10.1002/joc.5437

Kalnay, E., Kanamitsu, M., Kistler, R., Collins, W., Deaven, D., Gandin, L., et al. (1996). The NCEP/NCAR 40-year reanalysis project. *Bulletin of the American Meteorological Society*, *77*(3), 437–471. https://doi.org/10.1175/1520-0477(1996)077<0437:TNYRP>2.0.CO;2

Kao, H.-Y., & Yu, J.-Y. (2009). Contrasting eastern-Pacific and central-Pacific types of ENSO. *Journal of Climate*, *22*(3), 615–632. https://doi.org/10.1175/2008jcli2309.1

Kim, H.-M., Webster, P. J., & Curry, J. A. (2011). Modulation of north Pacific tropical cyclone activity by three phases of ENSO. *Journal of Climate*, *24*(6), 1839–1849. https://doi.org/10.1175/2010jcli3939.1

Kosaka, Y., Xie, S.-P., Lau, N.-C., & Vecchi, G. A. (2013). Origin of seasonal predictability for summer climate over the Northwestern Pacific. *Proceedings of the National Academy of Sciences*, *110*(19), 7574–7579. https://doi.org/10.1073/pnas.1215582110

Kug, J.-S., Jin, F.-F., & An, S.-I. (2009). Two types of El Niño events: Cold tongue El Niño and warm pool El Niño. *Journal of Climate*, *22*(6), 1499–1515. https://doi.org/10.1175/2008jcli2624.1

Li, R. C. Y., & Zhou, W. (2013). Modulation of western north Pacific tropical cyclone activity by the ISO. Part I: Genesis and intensity. *Journal of Climate*, *26*(9), 2904–2918. https://doi.org/10.1175/jcli-d-12-00210.1

19448007, 2021, 14, Downloaded from https://agupubs.onlinelibrary.wiley.com/doi/10.1029/2021GL094578 by CochraneChina, Wiley Online Library on [14/11/2026]. See the Terms and Conditions (https://onlinelibrary.wiley.com/terms-and-conditions) on Wiley Online Library for rules of use; OA articles are governed by the applicable Creative Commons License

Li, R. C. Y., & Zhou, W. (2018). Revisiting the intraseasonal, interannual and interdecadal variability of tropical cyclones in the western North Pacific. *Atmospheric and Oceanic Science Letters*, *11*(2), 198–208. https://doi.org/10.1080/16742834.2018.1459460
Liebmann, B., & Smith, C. A. (1996). Description of a complete (interpolated) outgoing longwave radiation dataset. *Bulletin of the American Meteorological Society*, *77*, 1275–1277. https://doi.org/10.1175/1520-0477-77.1.fmi
Madden, R. A., & Julian, P. R. (1971). Detection of a 40–50 day oscillation in the zonal wind in the tropical Pacific. *Journal of the Atmospheric Sciences*, *28*(5), 702–708. https://doi.org/10.1175/1520-0469(1971)028<0702:doadoi>2.0.co;2
Maloney, E. D., & Hartmann, D. L. (2001). The Madden–Julian oscillation, barotropic dynamics, and north Pacific tropical cyclone formation. Part I: Observations. *Journal of the Atmospheric Sciences*, *58*(17), 2545–2558. https://doi.org/10.1175/1520-0469(2001)058<2545:tmjobd>2.0.co;2
Moon, J.-Y., Wang, B., Lee, S.-S., & Ha, K.-J. (2018). An intraseasonal genesis potential index for tropical cyclones during northern hemisphere summer. *Journal of Climate*, *31*(22), 9055–9071. https://doi.org/10.1175/jcli-d-18-0515.1
Ren, H.-L., & Jin, F.-F. (2011). Niño indices for two types of ENSO. *Geophysical Research Letters*, *38*(4). https://doi.org/10.1029/2010gl046031
Stuecker, M. F., Timmermann, A., Jin, F.-F., McGregor, S., & Ren, H.-L. (2013). A combination mode of the annual cycle and the El Niño/southern oscillation. *Nature Geoscience*, *6*(7), 540–544. https://doi.org/10.1038/ngeo1826
Takaya, Y., Ishikawa, I., Kobayashi, C., Endo, H., & Ose, T. (2020). Enhanced Meiyu-Baiu rainfall in early summer 2020: Aftermath of the 2019 super IOD event. *Geophysical Research Letters*, *47*(22). https://doi.org/10.1029/2020gl090671
Wang, B., & Chan, J. C. L. (2002). How strong ENSO events affect tropical storm activity over the western north Pacific. *Journal of Climate*, *15*(13), 1643–1658. https://doi.org/10.1175/1520-0442(2002)015<1643:hseeat>2.0.co;2
Wang, B., Chen, G., & Liu, F. (2019). Diversity of the Madden-Julian Oscillation. *Science Advances*, *5*(7), eaax0220. https://doi.org/10.1126/sciadv.aax0220
Wang, B., Xiang, B., & Lee, J.-Y. (2013). Subtropical High predictability establishes a promising way for monsoon and tropical storm predictions. *Proceedings of the National Academy of Sciences*, *110*(8), 2718–2722. https://doi.org/10.1073/pnas.1214626110
Wang, C., Wang, B., & Wu, L. (2018). Abrupt breakdown of the predictability of early season typhoon frequency at the beginning of the twenty-first century. *Climate Dynamics*, *52*(7–8), 3809–3822. https://doi.org/10.1007/s00382-018-4350-9
Wang, C., Wu, K., Wu, L., Zhao, H., & Cao, J. (2021). What caused the unprecedented absence of western north Pacific tropical cyclones in July 2020? *Geophysical Research Letters*, *48*(9). https://doi.org/10.1029/2020gl092282
Wang, C., Yao, Y., Wang, H., Sun, X., & Zheng, J. (2021). The 2020 summer floods and 2020/21 winter extreme cold surges in China and the 2020 typhoon season in the western north Pacific. *Advances in Atmospheric Sciences*, *38*(6), 896–904. https://doi.org/10.1007/s00376-021-1094-y
Wang, X., Xie, S.-P., & Guan, Z. (2020). Atmospheric internal variability in the summer Indo–Northwestern Pacific: Role of the intraseasonal oscillation. *Journal of Climate*, *33*(8), 3395–3410. https://doi.org/10.1175/jcli-d-19-0794.1
Wheeler, M. C., & Hendon, H. H. (2004). An all-season real-time multivariate MJO index: Development of an index for monitoring and prediction. *Monthly Weather Review*, *132*(8), 1917–1932. https://doi.org/10.1175/1520-0493(2004)132<1917:aarmmi>2.0.co;2
Xie, S.-P., Hu, K., Hafner, J., Tokinaga, H., Du, Y., Huang, G., & Sampe, T. (2009). Indian Ocean capacitor effect on Indo–Western pacific climate during the summer following El Niño. *Journal of Climate*, *22*(3), 730–747. https://doi.org/10.1175/2008jcli2544.1
Yang, J., Liu, Q., Xie, S.-P., Liu, Z., & Wu, L. (2007). Impact of the Indian Ocean SST basin mode on the Asian summer monsoon. *Geophysical Research Letters*, *34*(2). https://doi.org/10.1029/2006gl028571
Zhan, R., Wang, Y., & Liu, Q. (2017). Salient differences in tropical cyclone activity over the western north Pacific between 1998 and 2016. *Journal of Climate*, *30*(24), 9979–9997. https://doi.org/10.1175/jcli-d-17-0263.1
Zhan, R., Wang, Y., & Wu, C.-C. (2011). Impact of SSTA in the east Indian Ocean on the frequency of northwest Pacific tropical cyclones: A regional atmospheric model study. *Journal of Climate*, *24*(23), 6227–6242. https://doi.org/10.1175/jcli-d-10-05014.1
Zhang, C., & Dong, M. (2004). Seasonality in the Madden-Julian oscillation. *Journal of Climate*, *17*(16), 3169–3180. https://doi.org/10.1175/1520-0442(2004)017<3169:SITMO>2.0.CO;2
Zhang, W., Huang, Z., Jiang, F., Stuecker, M. F., Chen, G., & Jin, F. (2021). Exceptionally persistent Madden-Julian oscillation activity contributes to the extreme 2020 east Asian summer monsoon rainfall. *Geophysical Research Letters*, *48*(5). https://doi.org/10.1029/2020gl091588
Zhang, W., Li, H., Jin, F.-F., Stuecker, M. F., Turner, A. G., & Klingaman, N. P. (2015). The annual-cycle modulation of meridional asymmetry in ENSO's atmospheric response and its dependence on ENSO zonal structure. *Journal of Climate*, *28*(14), 5795–5812. https://doi.org/10.1175/jcli-d-14-00724.1
Zhou, Z.-Q., Xie, S.-P., & Zhang, R. (2021). Historic Yangtze flooding of 2020 tied to extreme Indian Ocean conditions. *Proceedings of the National Academy of Sciences*, *118*(12), e2022255118. https://doi.org/10.1073/pnas.2022255118

19448007, 2021, 14, Downloaded from https://agupubs.onlinelibrary.wiley.com/doi/10.1029/2021GL094578 by CochraneChina, Wiley Online Library on [14/11/2026]. See the Terms and Conditions (https://onlinelibrary.wiley.com/terms-and-conditions) on Wiley Online Library for rules of use; OA articles are governed by the applicable Creative Commons License